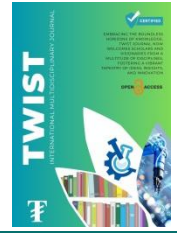# TWIST

Journal homepage: www.twistjournal.net

Modeling and Simulation of Blood Flow through an Inclined Artery with a Tapered Angle

Kubugha Wilcox Bunonyo*

Department of Mathematics and Statistics, Federal University Otuoke, Bayelsa, Nigeria

[*Corresponding author]

Liberty Ebiwareme

Department of Mathematics, Rivers State University, Port Harcourt, Nigeria

Abstract

The modeling and simulation of blood flow through an inclined artery with a tapering angle is the primary focus of this study. A mathematical model is developed to capture the dynamics of blood flow in this specific geometry. The dependable Homotopy perturbation method is employed to solve the governing equations, and the results are visually presented and analyzed. The study includes a comprehensive problem formulation, a solution strategy, graphical representation of simulated results, a quantitative examination of control parameters, and a summary of key conclusions. This research contributes to a better understanding of blood flow behavior in arteries with inclined and tapered geometries, which has implications for cardiovascular health and medical interventions.

Keywords

Chemical reaction, Magnetic field, Tapered angle, MHD, Inclined artery, Blood, Modeling, Simulation, Flow

INTRODUCTION

The complex mechanism of blood flow via various body components and through different limiting environments has long fascinated scholars. Given that blood is the body's essential force, knowing how it works and what stops it from flowing freely is crucial to the body's optimal operation. Blood flow is essential for maintaining homeostasis and facilitating optimal interaction among the body's organs as it carries nutrients, waste products, hormones, and other compounds throughout the body, McDonald [1]. Similar to this, the body needs blood for several processes, such as temperature regulation, cellular infection defense, fluid balance, and oxygen transport. Researchers have given a great deal of time to studying this innate curiosity and have developed several mathematical models to theoretically comprehend its complex origin. Numerous factors, including pressure gradients, tube diameters, artery radii, and frequency of body acceleration, as well as pulsatile pressure gradients caused by heart action, stress, flow resistance, and flow rate, have been identified from the literature as either slowing down or completely inhibiting blood flow through the body, Watanabe and Shintao [2]. The condition of poor blood flow regulation is referred to as ischemia or hypoperfusion in the medical profession. This situation, where there is almost no blood flow, could be fatal for the body if transfusions from another source are not administered, Tanaka et al. [3].

Several studies in contemporary literature have modeled and simulated the flow characteristics of blood through an inclined artery with a tapered angle, considering various parameters. Vasu et al. [4] simulated two-dimensional rheological laminar hemodynamics via a mildly stenotic diseased tapering artery and considered the potential use of metallic nanoparticles floating in the blood for drug administration. Majekodunmi et al. [5] investigated numerically the impact of tapering on blood flow via a stenosed artery using a non-Newtonian model. They discovered that while the radial velocity, wall shear stress, and flow resistance decrease, the flow rate and axial velocity rise as the tapering angle increases. Driver examined the impact of the bifurcation angle on flow factors in bifurcated arteries. [6]. It was observed that an increase in bifurcation angle led to an increase in recirculation, resulting in constriction of blood flow and an increased pressure gradient. In a study by Haghighi et al. [7], pulsatile blood flow through a tapered artery with a non-symmetric stenosis was simulated, and the flow characteristics were compared between elastic and inelastic arteries.

Srivastava [8] investigated pulsatile blood flow through an inclined stenosed artery using the Herschel-Bulkley model and derived an exact solution for the flow characteristics.

A simulated non-symmetric stenosis in a tapering artery was the subject of a two-dimensional model of pulsatile blood flow explored by Reza et al. [9]. With an axially non-symmetric stenosis and a time-dependent geometry, the blood flow measured as a cross fluid is represented in an elastic cylindrical tube. Within elastic and inelastic arteries, the blood flow velocities are contrasted. The governing equations are simplified through the use of a mild stenosis approximation. with the use of a suitable coordinate transformation. Using the Bessel function, Chitra et al. [10] observed the analytical solution to the mathematical modeling of unsteady MHD oscillatory blood flow in an inclined tapering stenosed artery with a permeable wall. The combined effects of thermal radiation and a magnetic field on blood flow in an inclined, tapering, stenosed porous artery have been studied by Abubakar and Adeoye [11]. Bakheet al. [12] implemented the blood flow for laminar, unsteady, and incompressible flow through a flexible stenosed artery utilizing the Marker and cell numerical technique in conjunction with the successive over-relaxation for the pressure gradient.

The impact of a heat source and magnetic field on blood flow through an inclined tapered channel has been investigated by Bunonyo and Ebiwareme [13] using the series approach. According to the study's findings, heat sources aid in blood circulation, while magnetic fields increase blood velocity. Analysis of the blood flow characteristics through an inclined tapered porous artery with minor stenosis under the influence of an inclined magnetic field has been addressed by Srivastava [14]. Using the homotopy perturbation method, Tripathi and Sharma [15] have addressed the issues of changing viscosity, magnetohydrodynamic effects, and chemical reaction on inclined arterial blood flow. Bunonyo et al. [16] have looked at the mathematical modeling of blood flow via a stenosed artery with heat in the presence of a magnetic field. Bunonyo and Ebiwareme [17] examined the influence of modeling inclined angles and magneto-hydrodynamics on blood flow through a gradient-tapered vessel. Their findings indicated that magnetic fields tend to increase blood flow velocity. Additionally, Bunonyo and Ebiwareme [18] discussed the theoretical evaluation of a magnetic and conducting fluid flow through a blood vessel, considering factors such as inclination and chemical reaction.

The Homotopy Perturbation Method (HPM) is a semi-analytical technique devised by Ji-Huan He in the late 1990s, known for its effectiveness in solving linear and nonlinear differential equations. Its popularity has grown due to its versatility, ease of use, and ability to tackle complex mathematical problems that are challenging for traditional analytical or numerical methods. The HPM is based on the concept of homotopy, which involves transforming a complicated differential equation into a simpler one called a homotopy equation. This method excels at handling a wide range of problems, including linear and nonlinear differential equations as well as partial differential equations. It is particularly adept at dealing with systems that have diverse initial conditions, boundary settings, and variable coefficients. Its flexibility in handling singularities or abrupt changes in values makes it indispensable in the fields of science and engineering. The HPM demonstrates excellent convergence characteristics, ensuring rapid and accurate convergence of the solution. The auxiliary parameter can be adjusted to control the convergence of the series solution. Overall, the HPM surpasses traditional perturbation techniques by providing precise solutions, even for highly nonlinear systems. It has been successfully applied to a multitude of scientific and technical challenges, with applications found in control systems, biology, physics, mechanics, and finance. Problems involving heat transfer, fluid dynamics, population dynamics, nonlinear oscillations, and various other topics have been resolved using the HPM. Furthermore, advancements in the HPM have expanded its applications, such as the fractional order HPM, which allows for the solution of fractional differential equations. The studies highlighted below provide detailed applications of HPM to a variety of problems across various disciplines [19–36].

This study focuses on the formulation of a mathematical model to simulate the dynamics of blood flow through a tapered artery. The efficient homotopy perturbation method is employed to solve the equations that describe the flow fields. The obtained results are visually presented and thoroughly analysed. The research is organized into several sections: Section 2 presents the problem formulation, considering all relevant assumptions. In Section 3, the solution strategy for the non-dimensional governing equation is explained. The subsequent section showcases the graphical representation of the simulated results for various parameters. Section 5 offers a quantitative analysis of the results obtained, considering the variation in control parameters. Finally, Section 6 provides a comprehensive summary of the study's main conclusions.

MATHEMATICAL FORMULATIONS

Let us consider the fluid to be non-Newtonian, incompressible, electrically conducting, and flowing through an inclined artery with a tapered angle α. In addition, the flow is driven by the temperature and the specie concentration difference, where they were affected by inclination at angles α_2 and α_3. The wall of the artery was considered porous and allows the passage of magnetic field which affects the moving electrically conducting fluid. The original models depicting the fluid flow through a tapered and inclined artery follows those used by Srivastava [8], and Bunonyo and Ebiwareme [13]. The momentum equation is presented as:

$$\rho \vec{F} = -\frac{\partial P^*}{\partial z^*} + \mu \left(\frac{\partial^2 u^*}{\partial r^{*2}} + \frac{1}{r^*} \frac{\partial u^*}{\partial r^*} \right) - \frac{\mu u^*}{k^*} + \vec{J} \times \vec{B} \qquad (1)$$

According to Darcy's law, the blood velocity is:

$$u^* = -\frac{k^*}{\mu}\frac{\partial P^*}{\partial z^*} \tag{2}$$

According to Bunonyo and Ebiwareme [13], the current density and magnetic field relation is given as:

$$\vec{J}\times\vec{B} = \sigma\left(\vec{E}+\vec{u}\times\vec{B}\right)\times\vec{B} \tag{3}$$

$$\beta_T = -\frac{1}{\rho}\left(\frac{\rho-\rho_\infty}{T^*-T_\infty}\right) \tag{4}$$

Substituting equations (2)-(4) into equation (1), we have the modified momentum equation as:

$$\rho g sin\alpha = -\frac{\partial P^*}{\partial x^*}+\mu\left(\frac{\partial^2 u^*}{\partial r^{*2}}+\frac{1}{r^*}\frac{\partial u^*}{\partial r^*}\right)+\rho\beta_T\left(T^*-T_\infty\right)cos\alpha_2+\rho\beta_c\left(C^*-C_\infty\right)sin\alpha_3-\frac{\mu u^*}{k^*}-\sigma B_0^2 u^* \tag{5}$$

In order to investigate the impact of the temperature and specie concentration differences on the fluid flow, we introduce the energy equation with a source according to Bunonyo and Amos [16] as:

$$\rho c_p\frac{\partial T^*}{\partial t^*} = k_T\left(\frac{\partial^2 T^*}{\partial r^{*2}}+\frac{1}{r^*}\frac{\partial T^*}{\partial r^*}\right)+Q_0\left(T^*-T_\infty\right) \tag{6}$$

$$\frac{\partial C^*}{\partial t^*} = k_T\left(\frac{\partial^2 C^*}{\partial r^{*2}}+\frac{1}{r^*}\frac{\partial C^*}{\partial r^*}\right)-Kr\left(C^*-C_\infty\right) \tag{7}$$

Equations (5)-(7) are subject to the following boundary conditions:

$$\left.\begin{array}{l}u^*=0, T^*=T_w, C^*=C_w \qquad \text{at } r^*=h^* \\[2mm] \dfrac{\partial u^*}{\partial r^*}=0, T^*=T_\infty, C^*=C_\infty \quad \text{at } r^*=0\end{array}\right\} \tag{8}$$

The dimensionless parameters are:

$$\left.\begin{array}{l}z^*=\dfrac{z}{d}, r^*=\dfrac{r}{d_0}, h^*=\dfrac{h}{d_0}, \upsilon^*=\dfrac{b\upsilon}{\delta u}, u^*=\dfrac{u}{u_0}, k^*=\dfrac{k}{d_0^2}, P^*=\dfrac{Pd_0^2}{d\mu\mu_0}, t^*=\dfrac{\upsilon t}{d_0^2}, \\[3mm] Fr=\dfrac{u_0^2}{gd_0}, M=\dfrac{\sigma d_0^2 B_0^2}{\mu}, Re=\dfrac{\rho u_0 d_0}{\mu}, \theta=\dfrac{T^*-T_\infty}{T_w-T_\infty}, \phi=\dfrac{C^*-C_\infty}{C-T_w}, Rd=\dfrac{Q_0 d_0^2}{\mu c_p}, \\[3mm] Gr=\dfrac{d_0^2\beta_T\left(T_w-T_\infty\right)}{\upsilon u_0}, Gc=\dfrac{d_0^2\beta_c\left(C-C_w\right)}{\upsilon u_0}, Pr=\dfrac{\mu c_p}{k_T}, Rd_0=\dfrac{Krd_0^2}{\upsilon}, Sc=\dfrac{\upsilon}{D_m}\end{array}\right\} \tag{9}$$

Using equation (8), the momentum and energy equations (5) to (7) reduce to the form.

$$\frac{Re}{Fr}sin\alpha = \frac{\partial^2 u}{\partial r^2}+\frac{1}{r}\frac{\partial u}{\partial r}-\left(\frac{1}{k}+M^2 cos^2\alpha_1\right)u+\theta Gr cos\alpha_2+\phi Gc sin\alpha_3 \tag{10}$$

$$Pr\frac{\partial\theta}{\partial t} = \frac{\partial^2\theta}{\partial r^2}+\frac{1}{r}\frac{\partial\theta}{\partial r}+Rd Pr\theta \tag{11}$$

$$Sc\frac{\partial\phi}{\partial t} = \frac{\partial^2\phi}{\partial r^2}+\frac{1}{r}\frac{\partial\phi}{\partial r}+Rd_0 Sc\phi \tag{12}$$

Equations (9)-(12) are subjected to the following boundary conditions:

$$\left.\begin{array}{l}u=0, \theta=1, \phi=1 \qquad \text{at } r=h \\[2mm] \dfrac{\partial u}{\partial r}=0, \theta=0, \phi=0 \qquad \text{at } r=0\end{array}\right\} \tag{13}$$

Since we considered the blood flow to be steady, $\dfrac{\partial\theta}{\partial t}=0$ and $\dfrac{\partial\phi}{\partial t}=0$, then equations (10)-(13) reduces to the following:

$$\frac{Re}{Fr}sin\alpha = \frac{\partial^2 u}{\partial r^2}+\frac{1}{r}\frac{\partial u}{\partial r}-\beta^2 u+\theta Gr cos\alpha_2+\phi Gc sin\alpha_3 \tag{14}$$

$$\frac{\partial^2\theta}{\partial r^2}+\frac{1}{r}\frac{\partial\theta}{\partial r}+\beta_2^2\theta = 0 \tag{15}$$

$$\frac{\partial^2 \phi}{\partial r^2} + \frac{1}{r}\frac{\partial \phi}{\partial r} + \beta_3^2 \phi = 0 \tag{16}$$

Equations (9)-(12) are subjected to the following boundary conditions:

$$\left. \begin{array}{l} u = 0, \theta = 1, \phi = 1 \qquad \text{at } r = h \\[2mm] \dfrac{\partial u}{\partial r} = 0, \theta = 0, \phi = 0 \qquad \text{at } r = 0 \end{array} \right\} \tag{17}$$

$$\text{where } \beta^2 = \left(\frac{1}{k} + M^2 cos^2\alpha_1 \right), \beta_2^2 = RdPr, \beta_3^2 = Rd_0Sc$$

Mathematical Application of Homotopy

In order to solve equations (15)-(18) using the Homotopy Method (HPM), we construct homotopies as follows:

$$\left. \begin{array}{l} H(u, p): \Omega \times [0,1] \to R \\[1mm] H(\theta, p): \Omega \times [0,1] \to R \\[1mm] H(\phi, p): \Omega \times [0,1] \to R \end{array} \right\} \tag{18}$$

which satisfies:

$$\begin{array}{l} H(u, p) = (1-p)[L(u) - L(u_0)] + p[L(u) + N(u) - f(r)] = 0 \\[2mm] H(\theta, p) = (1-p)[L(\theta) - L(\theta_0)] + p[L(\theta) + N(\theta) - f(r)] = 0 \\[2mm] H(\phi, p) = (1-p)[L(\phi) - L(\phi_0)] + p[L(\phi) + N(\phi) - f(r)] = 0 \end{array} \tag{19}$$

where $p \in [0,1]$, $f(r)$ is a known analytical function, L and N is linear and nonlinear functions.

Equations (19), which can be written in power series as:

$$u(r,t) = \sum_{n=0}^{\infty} p^n u_n(r,t) = u_0 + u_1 p + u_2 p^2 + \dots \tag{20}$$

$$\theta(r,t) = \sum_{n=0}^{\infty} p^n \theta_n(r,t) = \theta_0 + \theta_1 p + \theta_2 p^2 + \dots \tag{21}$$

$$\phi(r,t) = \sum_{n=0}^{\infty} p^n \phi_n(r,t) = \phi_0 + \phi_1 p + \phi_2 p^2 + \dots \tag{22}$$

Equations (20)-(22) can be differentiated as:

$$\frac{1}{r}\frac{\partial u}{\partial r} = \frac{1}{r}\frac{\partial u_0}{\partial r} + p\frac{1}{r}\frac{\partial u_1}{\partial r} + p^2\frac{1}{r}\frac{\partial u_2}{\partial r} + \dots \tag{23}$$

$$\frac{1}{r}\frac{\partial \theta}{\partial r} = \frac{1}{r}\frac{\partial \theta_0}{\partial r} + p\frac{1}{r}\frac{\partial \theta_1}{\partial r} + p^2\frac{1}{r}\frac{\partial \theta_2}{\partial r} + \dots \tag{24}$$

$$\frac{1}{r}\frac{\partial \phi}{\partial r} = \frac{1}{r}\frac{\partial \phi_0}{\partial r} + p\frac{1}{r}\frac{\partial \phi_1}{\partial r} + p^2\frac{1}{r}\frac{\partial \phi_2}{\partial r} + \dots \tag{25}$$

Equations (23)-(25) can be differentiated as:

$$\frac{\partial^2 u}{\partial r^2} = \frac{\partial^2 u_0}{\partial r^2} + p\frac{\partial^2 u_1}{\partial r^2} + p^2\frac{\partial^2 u_2}{\partial r^2} + \dots \tag{26}$$

$$\frac{\partial^2 \theta}{\partial r^2} = \frac{\partial^2 \theta_0}{\partial r^2} + p\frac{\partial^2 \theta_1}{\partial r^2} + p^2\frac{\partial^2 \theta_2}{\partial r^2} + \dots \tag{27}$$

$$\frac{\partial^2 \phi}{\partial r^2} = \frac{\partial^2 \phi_0}{\partial r^2} + p\frac{\partial^2 \phi_1}{\partial r^2} + p^2\frac{\partial^2 \phi_2}{\partial r^2} + \dots \tag{28}$$

We shall construct the Homotopy of equations (14)-17), we have the following:

$$H(\theta, 0) = L(\theta) - L(\theta_0) = \frac{\partial^2 \theta}{\partial r^2} - \frac{\partial^2 \theta_0}{\partial r^2} = 0 \tag{29}$$

$$H(\theta, 1) = L(\theta) + N(\theta) - f(r) = \frac{\partial^2 \theta}{\partial r^2} + \frac{1}{r}\frac{\partial \theta}{\partial r} + \beta_2^2 \theta = 0 \tag{30}$$

$$H(\theta, p) = (1-p)\left(\frac{\partial^2 \theta}{\partial r^2} - \frac{\partial^2 \theta_0}{\partial r^2} \right) + p\left(\frac{\partial^2 \theta}{\partial r^2} + \frac{1}{r}\frac{\partial^2 \theta}{\partial r^2} + \beta_2^2 \theta \right) = 0 \tag{31}$$

$$H(\theta, p) = \left\{ \begin{array}{l} \left[\left(p\dfrac{\partial^2 \theta_1}{\partial r^2} + p^2 \dfrac{\partial^2 \theta_2}{\partial r^2} \right) - \left(p^2 \dfrac{\partial^2 \theta_1}{\partial r^2} + p^3 \dfrac{\partial^2 \theta_2}{\partial r^2} \right) \right. \\ \left. p\left(\dfrac{\partial^2 \theta_0}{\partial r^2} + \dfrac{1}{r}\dfrac{\partial \theta_0}{\partial r} + \beta_2^2 \theta_0 \right) + p^2 \left(\dfrac{\partial^2 \theta_1}{\partial r^2} + \dfrac{1}{r}\dfrac{\partial \theta_1}{\partial r} + \beta_2^2 \theta_1 \right) + p^3 \left(\dfrac{\partial^2 \theta_2}{\partial r^2} + \dfrac{1}{r}\dfrac{\partial \theta_2}{\partial r} + \beta_2^2 \theta_2 \right) \right] \end{array} \right\} = 0 \qquad (32)$$

$$p^0 : \frac{\partial^2 \theta}{\partial r^2} = 0; \frac{\partial^2 \phi}{\partial r^2} = 0; \frac{\partial^2 u}{\partial r^2} = 0 \qquad (33)$$

$$p^1 : \frac{\partial^2 \theta_1}{\partial r^2} + \frac{\partial^2 \theta_0}{\partial r^2} + \frac{1}{r}\frac{\partial \theta_0}{\partial r} + \beta_2^2 \theta_0 = 0 \qquad (34)$$

$$p^2 : \frac{\partial^2 \theta_2}{\partial r^2} + \frac{1}{r}\frac{\partial \theta_1}{\partial r} + \beta_2^2 \theta_1 = 0 \qquad (35)$$

$$p^3 : \frac{1}{r}\frac{\partial \theta_2}{\partial r} + \beta_2^2 \theta_2 = 0 \qquad (36)$$

Equations (33)-(36) are subjected to the following boundary conditions:

$$\left. \begin{array}{ll} \theta_0 = 1, \theta_1 = 1, \theta_2 = 1 & \text{at } r = h \\ \theta_0 = 0, \theta_1 = 0, \theta_2 = 0 & \text{at } r = 0 \end{array} \right\} \qquad (37)$$

Solving equations (33)-(36) subject to the boundary condition in equation (37), we have:

$$\theta_0(r) = \frac{r}{h} \qquad (38)$$

Differentiating equation (38), we have:

$$\theta_0(r) = \frac{r}{h}, \frac{\partial \theta_0}{\partial r} = \frac{1}{h}, \frac{\partial^2 \theta_0}{\partial r^2} = 0 \qquad (39)$$

Substitute equation (39) into equation (34), we have:

$$\frac{\partial^2 \theta_1}{\partial r^2} = -\frac{1}{hr} - \frac{\beta_2^2 r}{h}; \frac{\partial \theta_1}{\partial r} = -\frac{1}{h}\ln r - \frac{\beta_2^2 r^2}{2h} + c_1 \qquad (40)$$

Solving equation (40), we have:

$$\theta_1 = \frac{1}{h}(r - r\ln r) - \frac{\beta_2^2 r^3}{6h} + rc_1 + c_2 = \frac{1}{h}\left((r - r\ln r) - \frac{\beta_2^2 r^3}{6} \right) + rc_1 + c_2 \qquad (41)$$

Substituting equations (38) and (41) into equation (21), we have:

$$\theta(r,t) = \theta_0 + \theta_1 = \frac{r}{h} + \frac{1}{h}\left((r - r\ln r) - \frac{\beta_2^2 r^3}{6} \right) + rc_1 + c_2 \qquad (42)$$

Solving equation (42) using the boundary condition in equation (21), we have:

$$c_1 = \frac{1}{h}\left((\ln h - 1) + \frac{\beta_2^2 h^2}{6} \right) \qquad (43)$$

$$\theta(r,t) = \frac{r}{h} + \frac{1}{h}\left((r - r\ln r) - \frac{\beta_2^2 r^3}{6} \right) + \frac{r}{h}\left((\ln h - 1) + \frac{\beta_2^2 h^2}{6} \right) \qquad (44)$$

In a similar vein, we shall form the Homotopy equation for the concentration as:

$$H(\phi, 0) = L(\phi) - L(\phi_0) = \frac{\partial^2 \phi}{\partial r^2} - \frac{\partial^2 \phi_0}{\partial r^2} = 0 \qquad (45)$$

$$H(\phi, 1) = L(\phi) + N(\phi) - f(r) = \frac{\partial^2 \phi}{\partial r^2} + \frac{1}{r}\frac{\partial^2 \phi}{\partial r^2} + \beta_3^2 \phi = 0 \qquad (46)$$

$$H(\phi, p) = (1 - p)\left(\frac{\partial^2 \phi}{\partial r^2} - \frac{\partial^2 \phi_0}{\partial r^2} \right) + p\left(\frac{\partial^2 \phi}{\partial r^2} + \frac{1}{r}\frac{\partial \phi}{\partial r} + \beta_3^2 \phi \right) = 0 \qquad (47)$$

Substituting equations (22), (25), and (28) into equation (16) and (17), we have:

$$H(\phi, p) = \left\{ \begin{array}{l} \left(p\dfrac{\partial^2 \phi_1}{\partial r^2} + p^2 \dfrac{\partial^2 \phi_2}{\partial r^2} \right) - \left(p^2 \dfrac{\partial^2 \phi_1}{\partial r^2} + p^3 \dfrac{\partial^2 \phi_2}{\partial r^2} \right) \\ p\left(\dfrac{\partial^2 \phi_0}{\partial r^2} + \dfrac{1}{r}\dfrac{\partial \phi_0}{\partial r} + \beta_3^2 \phi_0 \right) + p^2 \left(\dfrac{\partial^2 \phi_1}{\partial r^2} + \dfrac{1}{r}\dfrac{\partial \phi_1}{\partial r} + \beta_3^2 \phi_1 \right) + p^3 \left(\dfrac{\partial^2 \phi_2}{\partial r^2} + \dfrac{1}{r}\dfrac{\partial \phi_2}{\partial r} + \beta_3^2 \phi_2 \right) \end{array} \right\} = 0 \qquad (48)$$

Resolving equation (52), we have:

$$p^0 : \frac{\partial^2 \phi}{\partial r^2} = 0 \tag{49}$$

$$p^1 : \frac{\partial^2 \phi_1}{\partial r^2} + \frac{\partial^2 \phi_0}{\partial r^2} + \frac{1}{r}\frac{\partial \phi_0}{\partial r} + \beta_3^2 \phi_0 = 0 \tag{50}$$

$$p^2 : \frac{\partial^2 \phi_2}{\partial r^2} + \frac{1}{r}\frac{\partial \phi_1}{\partial r} + \beta_2^2 \phi_1 = 0 \tag{51}$$

$$p^3 : \frac{1}{r}\frac{\partial \phi_2}{\partial r} + \beta_2^2 \phi_2 = 0 \tag{52}$$

Equations (53)-(56) are subjected to the following boundary conditions:

$$\left. \begin{array}{l} \phi_0 = 1, \phi_1 = 1 \quad \text{at} \quad r = h \\ \phi_0 = 0, \phi_1 = 0 \quad \text{at} \quad r = 0 \end{array} \right\} \tag{53}$$

Solving equations (53)-(56) subject to the boundary condition in equation (57), we have:

$$\phi_0(r) = \frac{r}{h} \tag{54}$$

Differentiating equation (58), we have:

$$\phi_0(r) = \frac{r}{h}, \frac{\partial \phi_0}{\partial r} = \frac{1}{h}, \frac{\partial^2 \phi_0}{\partial r^2} = 0 \tag{55}$$

Substitute equation (59) into equation (54), we have:

$$\frac{\partial^2 \phi_1}{\partial r^2} = -\frac{1}{hr} - \frac{\beta_3^2 r}{h}; \frac{\partial \phi_1}{\partial r} = -\frac{1}{h}\ln r - \frac{\beta_3^2 r^2}{2h} + c_3 \tag{56}$$

Solving equation (60), we have:

$$\phi_1 = \frac{1}{h}(r - r\ln r) - \frac{\beta_3^2 r^3}{6h} + rc_1 + c_2 = \frac{1}{h}\left((r - r\ln r) - \frac{\beta_3^2 r^3}{6} \right) + rc_3 + c_4 \tag{57}$$

Solving equation (40), we have:

$$\phi_1 = \frac{1}{h}(r - r\ln r) - \frac{\beta_3^2 r^3}{6h} + rc_1 + c_2 = \frac{1}{h}\left((r - r\ln r) - \frac{\beta_3^2 r^3}{6} \right) + rc_3 + c_4 \tag{58}$$

Substituting equations (38) and (41) into equation (21), we have:

$$\phi(r,t) = \phi_0 + \phi_1 = \frac{r}{h} + \frac{1}{h}\left((r - r\ln r) - \frac{\beta_3^2 r^3}{6} \right) + rc_3 + c_4 \tag{59}$$

Solving equation (42) using the boundary condition in equation (21), we have:

$$c_3 = \frac{1}{h}\left((\ln h - 1) + \frac{\beta_3^2 h^2}{6} \right) \tag{60}$$

$$\phi(r,t) = \frac{r}{h} + \frac{1}{h}\left((r - r\ln r) - \frac{\beta_3^2 r^3}{6} \right) + \frac{r}{h}\left((\ln h - 1) + \frac{\beta_3^2 h^2}{6} \right) \tag{61}$$

In a similar vein, we have:

$$\frac{Re}{Fr}\sin\alpha = \frac{\partial^2 u}{\partial r^2} + \frac{1}{r}\frac{\partial u}{\partial r} - \beta^2 u + \theta Gr\cos\alpha_2 + \phi Gc\sin\alpha_3 \tag{14}$$

$$H(u, p) = (1 - p)[L(u) - L(u_0)] + p[L(u) + N(u) - f(r)] = 0 \tag{62}$$

We shall construct the Homotopy of equations (14), we have the following:

$$H(u, 0) = L(u) - L(u_0) = \frac{\partial^2 u}{\partial r^2} - \frac{\partial^2 u_0}{\partial r^2} = 0 \tag{63}$$

$$H(u,1) = L(u) + N(u) - f(r) = \frac{\partial^2 u}{\partial r^2} + \frac{1}{r}\frac{\partial^2 u}{\partial r^2} - \beta_1^2 u - f(r) = 0 \tag{64}$$

$$H(u,p) = (1-p)\left(\frac{\partial^2 u}{\partial r^2} - \frac{\partial^2 u_0}{\partial r^2}\right) + p\left(\frac{\partial^2 u}{\partial r^2} + \frac{1}{r}\frac{\partial u}{\partial r} + \beta_1^2 u - \frac{Re}{Fr}\sin\alpha - \theta Gr\cos\alpha_2 - \phi G\sin\alpha_3\right) = 0 \tag{65}$$

Substituting equations (20), (23) and (26) into equation (65), we have:

$$H(u,p) = (1-p)\left(\frac{\partial^2 u_0}{\partial r^2} + p\frac{\partial^2 u_1}{\partial r^2} - \frac{\partial^2 u_0}{\partial r^2}\right) + p\left(\begin{array}{l}\dfrac{\partial^2 u_0}{\partial r^2} + p\dfrac{\partial^2 u_1}{\partial r^2} + \dfrac{1}{r}\dfrac{\partial u_0}{\partial r} + p\dfrac{1}{r}\dfrac{\partial u_1}{\partial r} - \beta_1^2(u_0 + u_1 p) \\[2mm] -\theta Gr\cos\alpha_2 - \phi G\sin\alpha_3 - \dfrac{Re}{Fr}\sin\alpha\end{array}\right) = 0 \tag{66}$$

$$H(u,p) = (1-p)\left(\frac{\partial^2 u_0}{\partial r^2} + p\frac{\partial^2 u_1}{\partial r^2} - \frac{\partial^2 u_0}{\partial r^2}\right) + p\left(\begin{array}{l}\dfrac{\partial^2 u_0}{\partial r^2} + p\dfrac{\partial^2 u_1}{\partial r^2} + \dfrac{1}{r}\dfrac{\partial u_0}{\partial r} + p\dfrac{1}{r}\dfrac{\partial u_1}{\partial r} - \beta_1^2(u_0 + u_1 p) \\[2mm] -(\theta_0 + \theta_1 p)Gr\cos\alpha_2 - (\phi_0 + \phi_1 p)G\sin\alpha_3 - \dfrac{Re}{Fr}\sin\alpha\end{array}\right) = 0 \tag{67}$$

$$\left(\begin{array}{l}p\dfrac{\partial^2 u_1}{\partial r^2} + p\dfrac{\partial^2 u_0}{\partial r^2} + p\dfrac{1}{r}\dfrac{\partial u_0}{\partial r} - \beta_1^2 u_0 p - p\theta_0 Gr\cos\alpha_2 - p\phi_0 G\sin\alpha_3 - \dfrac{pRe}{Fr}\sin\alpha \\[2mm] -p^2\dfrac{\partial^2 u_1}{\partial r^2} + p^2\dfrac{\partial^2 u_1}{\partial r^2} + p^2\dfrac{1}{r}\dfrac{\partial u_1}{\partial r} - \beta_1^2 u_1 p^2 - \theta_1 p^2 Gr\cos\alpha_2 - \phi_1 p^2 G\sin\alpha_3\end{array}\right) = 0 \tag{68}$$

$$p^0 : \frac{\partial^2 u}{\partial r^2} = 0 \tag{69}$$

$$p^1 : \frac{\partial^2 u_1}{\partial r^2} + \frac{\partial^2 u_0}{\partial r^2} + \frac{1}{r}\frac{\partial u_0}{\partial r} - \beta_1^2 u_0 - \theta_0 Gr\cos\alpha_2 - \phi_0 G\sin\alpha_3 - \frac{Re}{Fr}\sin\alpha = 0 \tag{70}$$

$$p^2 : \frac{1}{r}\frac{\partial u_1}{\partial r} - \beta_1^2 u_1 - \theta_1 Gr\cos\alpha_2 - \phi_1 G\sin\alpha_3 = 0 \tag{71}$$

Equations (69)-(71) are subjected to the following boundary conditions:

$$\left.\begin{array}{ll}u_0 = 0, u_1 = 0, \theta_0 = 1, \theta_1 = 1, \theta_2 = 1 & \text{at } r = h \\[2mm] \dfrac{\partial u_0}{\partial r} = 0, \dfrac{\partial u_1}{\partial r} = 0, \theta_0 = 0, \theta_1 = 0, \theta_2 = 0 & \text{at } r = 0\end{array}\right\} \tag{72}$$

From the boundary condition in equation (72), we have:

$$u_0 = \lambda, \theta_0 = \frac{r}{h}, \phi_0 = \frac{r}{h} \tag{73}$$

Solving equation (70) subject to the boundary conditions in equation (72), we have:

$$\frac{\partial^2 u_1}{\partial r^2} = \beta_1^2 \lambda + \frac{r}{h}Gr\cos\alpha_2 + \frac{r}{h}G\sin\alpha_3 + \frac{Re}{Fr}\sin\alpha \tag{74}$$

Simplifying equation (74), we have:

$$u_1 = \beta_1^2 \lambda \frac{r^2}{2} + \frac{r^3}{6h}Gr\cos\alpha_2 + \frac{r^3}{6h}G\sin\alpha_3 + \frac{r^2 Re}{2Fr}\sin\alpha + rc_5 \tag{75}$$

Simplifying equation (75) using the boundary condition in equation (72), we have:

$$u(r,t) = \lambda\left(1 - \frac{r}{h}\right) + \frac{\beta_1^2 \lambda}{2}(r^2 - hr) + \frac{r}{3}\left(\frac{r^2}{2h} - \frac{h}{2}\right)Gr\cos\alpha_2 + \frac{r}{3}\left(\frac{r^2}{2h} - \frac{h}{2}\right)G\sin\alpha_3 + \frac{rRe}{2Fr}(r - hr)\sin\alpha \tag{76}$$

RESULTS

Having solved the formulated models using HPM, the obtained blood velocity, temperature, specie concentration profiles were obtained. We used Wolfram Mathematica, version 12 to perform the numerical simulation where the pertinent parameters were varied to study their effect on the various flow profiles. The parameter values were obtained from previous research by Bunonyo and Ebiwareme [13], and the results are presented in the order of temperature, concentration, and velocity profiles respectively.
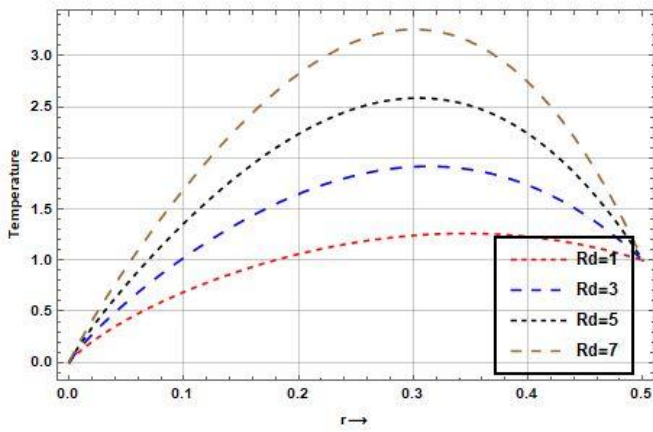
Temperature Profile

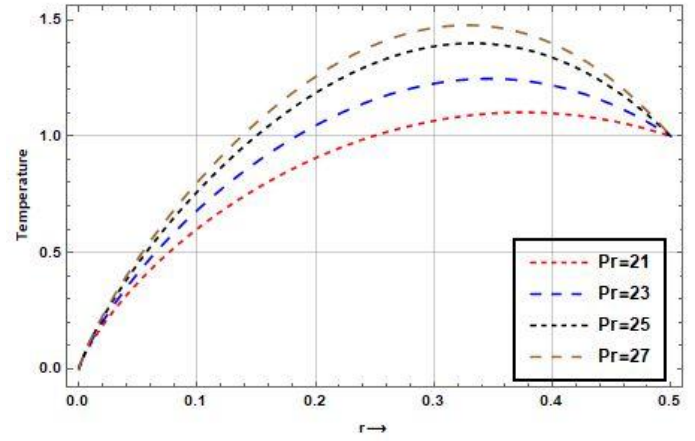**Fig. 1** Effect of radiation on temperature profile of the fluid

Fig. 2 Effect of Prandtl number on temperature profile of the fluid

Concentration Profile

The simulated specie concentration profile results for the reaction and Schmidt numbers are presented as follows:
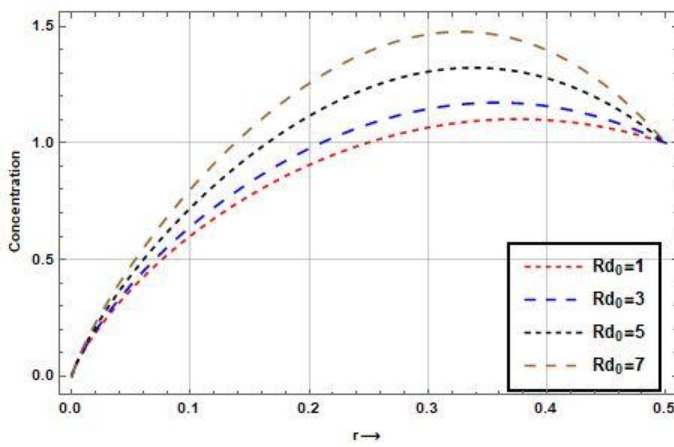

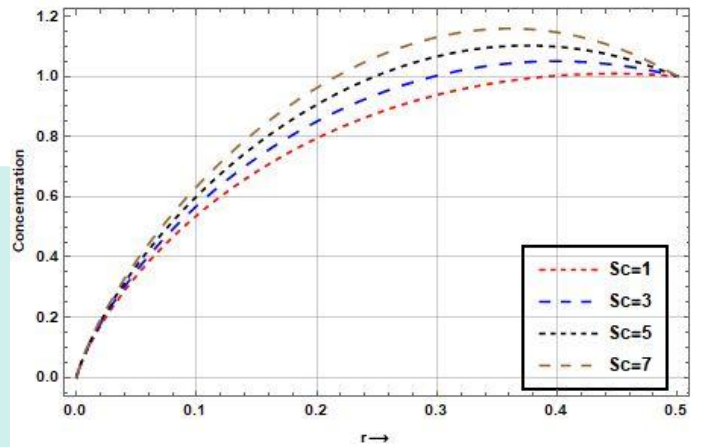**Fig. 3** Effect of chemical reaction on concentration profile of the fluid

Fig. 4 Effect of Schmidt number on the concentration profile of the fluid

Velocity Profile

The simulated results of the blood velocity profile can be presented for different varying pertinent parameters as follows:
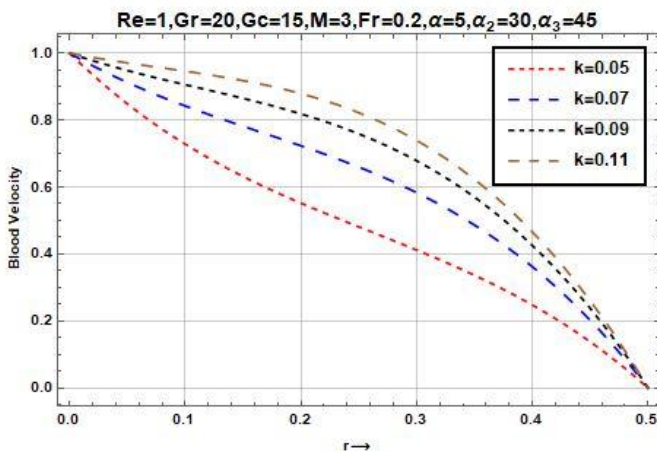

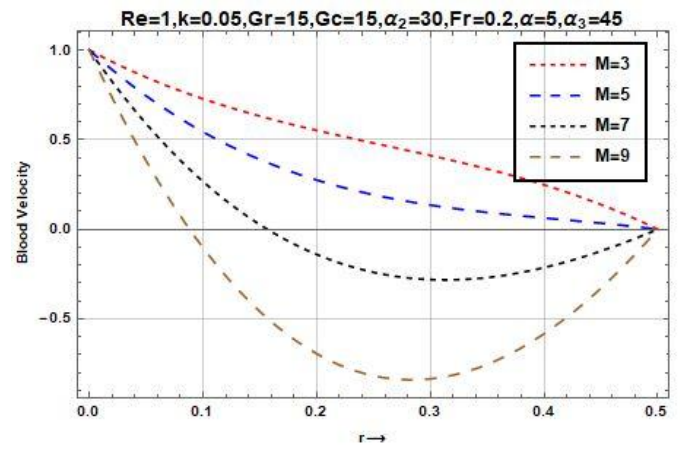**Fig. 5** Effect of Darcy number on the velocity profile of the fluid

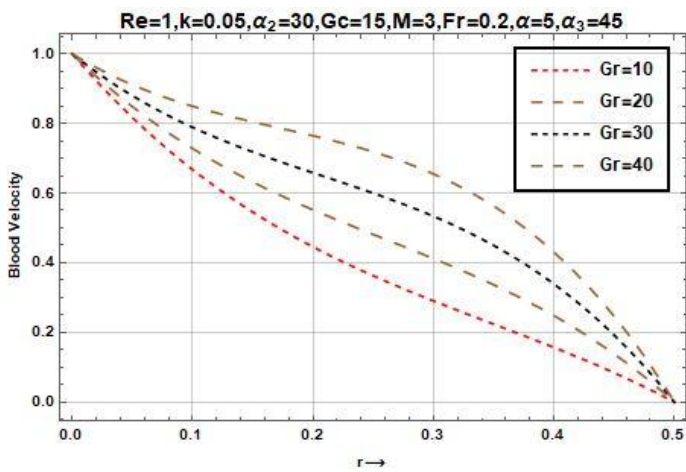**Fig. 6** Effect of magnetic field on the velocity profile of the fluid

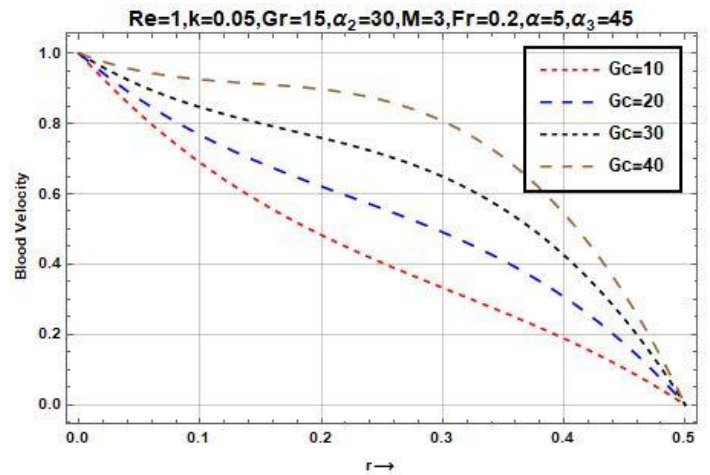**Fig. 7** Effect of thermal Grashof number on the velocity profile of the fluid

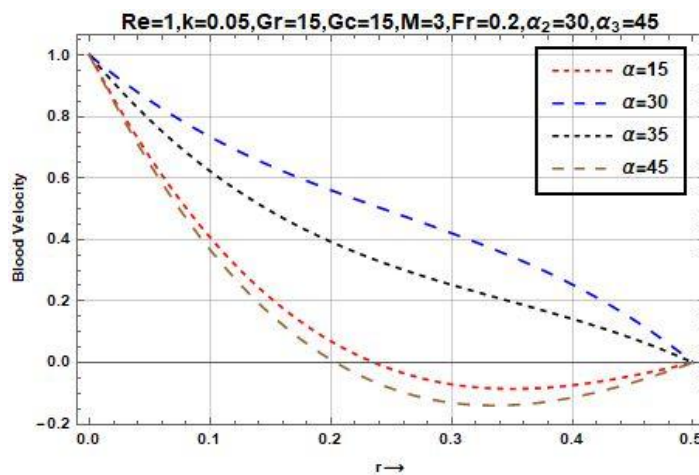**Fig. 8** Effect of solutal Grashof number on the velocity profile of the fluid

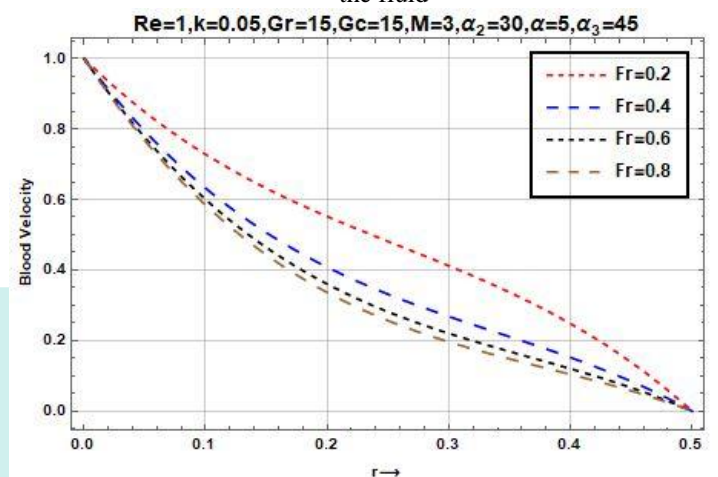**Fig. 9** Effect of tapered angle on the velocity profile of the fluid

Fig. 10 Effect of Froude number on the velocity profile of the fluid
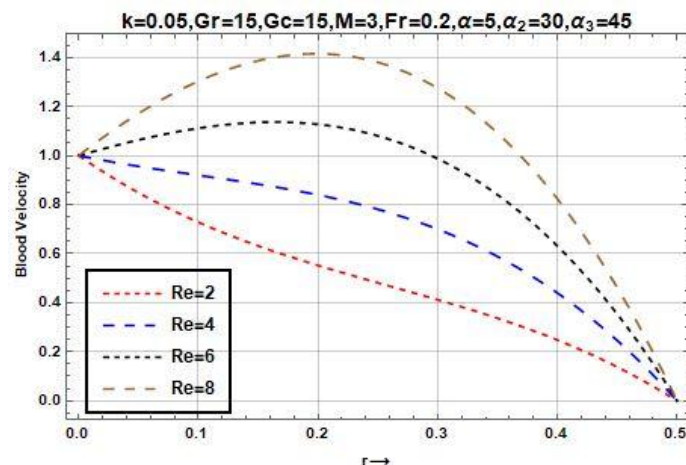

Fig. 11 Effect of Reynolds number on velocity profile of the fluid

DISCUSSION

Given the presentation of the simulated results in Section 4, we can discuss the results as follows: Figure 1 depicts the effect of radiation on the fluid temperature profile. The result shows that the temperature was at its peak at zero thickness at the walls of the artery; however, the temperature began to decrease as the boundary layer thickness increased and converged to zero at the maximum thickness of the boundary layer. Figure 2 illustrates that the increase in the Prandtl number causes a corresponding rise in fluid temperature. It was observed that the fluid temperature was maximum at zero wall thickness; however, the temperature began to decrease with increasing Prandtl values until it converged to zero at maximum thickness. In a similar vein, Figure 3 depicts the influence of the chemical reaction on the specie concentration in the fluid. The figure clearly illustrates that the concentration was minimal at the zero-wall thickness level; however, the concentration began to increase with an increase in chemical reaction along with the increase in the wall thickness until it reached a convergent concentration as the thickness attained a maximum. Figure 4 illustrates the influence of the Schmidt number on specie concentration in the fluid. The result is of the view that the specie concentration was zero at zero wall thickness for a specific Schmidt number value; however, the concentration increases for different values of the Schmidt number as the thickness level increases and converges at unity at the maximum wall thickness. The influence of the Darcy

number on the fluid velocity is presented in Figure 5. The result illustrates a maximum velocity at zero wall thickness on the walls of the artery. However, the increase in Darcy's number increases the velocity, but it decreases to zero at maximum thickness.

When a magnetic field comes into contact with a moving electrically conducting fluid, such as blood, it generates a force called the Lorentz force, which inhibits the velocity of the fluid, as depicted in Figure 6. The result is of the view that there was maximum velocity at zero wall thickness, but that velocity was observed to be decreasing for the increasing values of the magnetic field until it converged at zero velocity at maximum wall thickness. Figures 7 and 8 illustrate the influence of thermal Grashof and solutal Grashof numbers on the fluid velocity. The results showed maximum velocity at zero wall thickness but drastically increased with an increase in the Grashof and solutal Grashof numbers, respectively. However, the velocity decreases to zero at maximum wall thickness. The influence of the tapered angle on blood velocity was investigated, and the result confirmed maximum velocity at zero wall thickness, as illustrated in Figure 9. Figure 10 elucidates the influence of the Froude number on blood velocity and finds the velocity to be maximum at the zero-boundary layer thickness. In addition, the velocity profile decreases with an increase in the Froude number; however, the velocity decreases to zero as the thickness reaches its peak. Reynolds number influence was investigated as illustrated using Figure 11; the result showed a normal trend of maximum velocity at the zero-boundary layer thickness; however, we observed an increase in blood velocity for an increase in Reynolds number along the channel; the velocity attains zero at the maximum thickness.

CONCLUSION

Having carried out the research titled Modeling and Simulation of Blood Flow through an Inclined Artery with a Tapered Angle, with specific objectives achieved, we conclude as follows:
1. An increase in radiation and Prandtl number increases the fluid temperature.
2. The increase in chemical reaction and Schmidt number increases the specie concentration.
3. There is an increase in blood velocity for an increase in Darcy number.
4. A magnetic field increase decreases the velocity of the fluid.
5. The fluid velocity increases with an increase in thermal Grashof and solutal Grashof numbers.
6. The fluid velocity decreases with an increase in Froude number.
7. An increase in Reynolds' number caused a corresponding increase in fluid velocity.

REFERENCES
1. McDonald, D. A. (2022). Blood Flow in the Arteries: Theoretical, Experimental and Clinical Principles 7th Edition, CRC Press, New York.
2. Watanabe, T., Shintao, T. (2020). Blood flow measuring method for blood vessel identification.PharmocolToxicol Methods, 44(2):375-84., doi: 10.1016/s1056-8719(00)00123-4.
3. Tanaka, M., Ohta, T., & Hagiwara, Y. (2007). Motion of a thrombus in blood flow through a stenosed vessel. *Volume 1: Symposia, Parts A and B*. https://doi.org/10.1115/fedsm2007-37391
4. Vasuˈ B., Ankita, D., Anwar Bég, O., Rama Subba, R. G. (2020). Micropolar pulsatile blood flow conveying nanoparticles in a stenotic tapered artery: non-Newtonian pharmacodynamic simulation. Computers in Biology and Medicine (Elsevier)-Vol. 126, pp 104025.
5. Majekodunmi Joshua, T., Anwar, K., Nooraihan, A. (2020). Numerical Simulation of Non-Newtonian Blood Flow through a Tapered Stenosed Artery using the Cross Model. IOP Conf. Ser.: Mater. Sci. Eng. 864 012200 **DOI** 10.1088/1757-899X/864/1/012200.
6. Martha Driver, W. (2023). Numerical Simulation of Blood Flow Study in an Idealized Bifurcated Coronary Artery. Fluid Mechanics and Fluid Power, Vol. 2, pp 13–18.
7. Ahmad Reza, H, Pirhadi, N.,. Shahbazi, A. M (2019). A Mathematical modelling for the study of blood flow as a cross fluid through a tapered artery. Journal of Biomechanics, Volume 5, Issue 20, pp 15-30.
8. Srivastava, N. (2018). Herschel-Bulkley Magnetized Blood Flow Model for an inclined Tapered Artery for an Accelerated Body. Journal of Science and Technology, Volume. 10, Issue 1, pp. 53-59, DOI: https://10.30880/jst.2018.10.01.008.
9. Ahmad Reza, H., Mohammad, S, A., Mehdi, K. (2015). A Mathematical modeling for the study of blood flow as a cross fluid through a tapered artery. Journal of The Brazilian Society of Mechanical Sciences and Engineering, Volume 37, Issue: 2, pp 571-578.
10. Chitra, M., Parthasarathy, S., Karthikeyan, D. (2019). Mathematical Modelling on unsteady oscillatory flow of blood in an inclined tapered stenosed artery with permeable wall. *International Journal of Research in Advent Technology, Vol.7, No.1, January 2019 E-ISSN: 2321-9637*
11. Abubakar, J. U., Adeoye, A. D. (2020). Effects of radiative heat and magnetic field on blood flow in an inclined tapered stenosed porous artery. Journal of Taibah University for Science, Volume. 14, Issue: 1, pp 77-86.
12. Bakheet, A., Alnussaiyri, E. A.,, Zuhaila, I., Norsarahaida, A. (2016). Blood flow through an inclined stenosed artery. Applied mathematical sciences, Volume. 10, pp 235-254.
13. Bunonyo, K., & Ebiwareme, L. (2023). Influence of a magnetic Field on blood flow through an inclined tapered vessel with a heat source. *International Journal of Multidisciplinary Research and Analysis*, *06*(03). https://doi.org/10.47191/ijmra/v6-i3-32
14. Srivastava, N. (2014). Analysis of flow characteristics of the blood flowing through an inclined tapered porous artery with mild stenosis under the influence of an inclined magnetic Field. *Journal of Biophysics*, *2014*, 1-9. https://doi.org/10.1155/2014/797142.

15. Tripathi, B., & Sharma, B. (2018). Effect of variable viscosity on MHD inclined arterial blood flow with chemical reaction. *International Journal of Applied Mechanics and Engineering*, *23*(3), 767-785. https://doi.org/10.2478/ijame-2018-0042.

16. Bunonyo, K., Israel-Cookey, C., & Amos, E. (2018). Modelling of blood flow through stenosed artery with heat in the presence of magnetic Field. *Asian Research Journal of Mathematics*, *8*(1), 1-14. https://doi.org/10.9734/arjom/2018/37767

17. Bunonyo, K. W., Ebiwareme, L. (2023). Modeling and investigation of the influence of Angle of inclination on magnetohydrodynamics blood flow through a tapered vessel. Asian Journal of Pure and Applied Mathematics, Volume 5, Issue1, Pages 370-382, Article No: AJPAM 1377.

18. Bunonyo, K. W., Ebiwareme, L. (2023). Mathematical Analysis of a Magnetic and Conducting Fluid Flow through Blood Vessel Along with an Inclination and Chemical Reaction. European Journal of Theoretical and Applied Sciences, 1(6), 3-15, DOI: 10.59324/ejtas.2023.1(6).01

19. Abbasbandy, S. (2006). The application of homotopy perturbation method to nonlinear equations arising in heat transfer. Physics Letters A, 360(1), 109-113.

20. Jafari, H., & Daftardar-Gejji, V. (2006). Solving a system of nonlinear fractional differential equations using homotopy perturbation method. Journal of Computational and Applied Mathematics, 207(1), 24-34.

21. Ji-Huan, H. (2003). Homotopy perturbation method: a new nonlinear analytical technique, Applied Mathematics and Computation 135, 73-79.

22. Ji-Huan, H. (2009). An elementary introduction to the homotopy perturbation method, Computers and Mathematics with Applications 57, 410412.

23. Biazar, J., Ghazvini, H. (2007). Solution of the Wave Equation by Homotopy Perturbation Method, International Mathematical Forum, 2, no. 45, 2237 - 2244

24. Changbum, C., Hossein, J., Yong-Il, K. (2009). Numerical method for the wave and nonlinear diffusion equations with the homotopy perturbation method, Computers and Mathematics with Applications 57, 1226-1231.

25. Sadighi, A., Ganji, D. D. (2007). Exact solutions of Laplace equation by homotopy-perturbation and Adomian decomposition methods, Physics Letters A 367, 83-87.

26. Ghorbani, A., Saberi-Nadjafi, J. (2007). He's Homotopy Perturbation Method for Calculating Adomian Polynomials International Journal of Nonlinear Sciences ansd Numerical Simulation, 8(2), 229-232.

27. Yasir, K., Qingbiao, W. (2011). Homotopy perturbation transform method for nonlinear equations using He's polynomials, Computers and Mathematics with Applications, 61 1963-1967.

28. Mostafa, E., Jafar, B. (2014). Analytical solution of the Klein-Gordon Equation by A New homotopy perturbation method, computational mathematics and modeling, Vol. 25, No. 1,

29. Taghizadeh, N., Akbari, M., Ghelichzadeh, A. (2011). Exact Solution of Burgers Equations by Homotopy Perturbation Method and Reduced Differential Transformation Method, Australian Journal of Basic and Applied Sciences, 5(5): 580-589, ISSN 1991-8178.

30. Sadighi, A., Ganji, D. D. (2008). Analytic treatment of linear and nonlinear Schrödinger equations: A study with homotopy-perturbation and Adomian decomposition methods, Physics Letters A 372, 465-469.

31. Ahmet, Y. (2009). on the solution of the nonlinear Korteweg–de Vries equation by the homotopy perturbation method, Commun. Numer. Meth. Engng, 25:1127-1136.

32. Yildirim, A. (2008). The Homotopy Perturbation Method for Solving the Modified Korteweg-de Vries Equation, Z. Naturforsch. 63a, 621- 626.

33. Ebiwareme, L., Bunonyo, K. W. (2022). A New Homotopy perturbation-Sumudu Transform method Applied to Physical Models. International Research Journal of Modernization in Engineering Technology and Science, volume 4, Issue 11, November-2022.

34. Ebiwareme, L., Kormane, F. P. (2022). A variational Homotopy Perturbation method approach to the nonlinear equations governing MHD Jeffery-Hamel flow in the presence of magnetic field. American Journal of Engineering Research, Volume-11, Issue-02, pp-81-89.

35. Ebiwareme, L., Bunonyo, K. W., Davies, O. A. (2023). Homotopy Perturbation method for MHD Heat and Mass transfer flow of convective fluid through a vertical porous plate in the presence of chemical reaction and inclined magnetic field. Earthline Journal of Mathematical Sciences, Volume 13, Number 1, Pages 209-233.

36. Ganji, D. D. (2006). The Application of He's Homotopy Perturbation Method to Nonlinear Equations Arising in Heat Transfer. Physics Letters A, 355(4-5), 337-341.